

# The C terminus of p53 binds the N-terminal domain of MDM2

Masha V Poyurovsky<sup>1</sup>, Chen Katz<sup>3</sup>, Oleg Laptenko<sup>1</sup>, Rachel Beckerman<sup>1</sup>, Maria Lokshin<sup>1</sup>, Jinwoo Ahn<sup>2</sup>, In-Ja L Byeon<sup>2</sup>, Ronen Gabizon<sup>3</sup>, Melissa Mattia<sup>4</sup>, Andrew Zupnick<sup>1</sup>, Lewis M Brown<sup>1</sup>, Assaf Friedler<sup>3</sup> & Carol Prives<sup>1</sup>

**The p53 tumor suppressor interacts with its negative regulator Mdm2 via the former's N-terminal region and core domain, yet the extreme p53 C-terminal region contains lysine residues ubiquitinated by Mdm2 and can bear post-translational modifications that inhibit Mdm2-p53 association. We show that the Mdm2-p53 interaction is decreased upon deletion, mutation or acetylation of the p53 C terminus. Mdm2 decreases the association of full-length but not C-terminally deleted p53 with a DNA target sequence *in vitro* and in cells. Further, using multiple approaches, we show that a peptide from the p53 C terminus directly binds the Mdm2 N terminus *in vitro*. We also show that p300-acetylated p53 inefficiently binds Mdm2 *in vitro*, and Nutlin-3 treatment induces C-terminal modification(s) of p53 in cells, explaining the low efficiency of Nutlin-3 in dissociating p53-MDM2 *in vitro*.**

The tumor suppressor p53 is the focus of numerous investigations whose goal is reversing or halting tumor progression. The activity of p53 is tightly regulated in cells through post-translational modifications, localization and degradation<sup>1</sup>. The murine double minute (Mdm2) protein, a product of a p53-inducible gene, is a really interesting new gene (RING)-type E3 ubiquitin ligase responsible for proteasomal degradation of p53 (refs. 2,3). As an additional regulatory mechanism, Mdm2 binds directly to the first transactivation domain (TAD-I<sub>20–40</sub>) of p53, inhibiting its ability to interact with transcriptional coactivators<sup>4</sup>. X-ray crystallography and NMR studies have characterized the interaction between a hydrophobic pocket within the N-terminal region of Mdm2 and a peptide spanning the TAD-I domain of p53 (ref. 5). Biologically active inhibitors of this interaction (such as Nutlin-3) have been developed with the goal of dissociating p53 from Mdm2 and activating p53 in abnormally proliferating cells<sup>6–8</sup>.

Upon various forms of DNA damage, the TAD-I of p53 is modified by upstream protein kinases on several residues that weaken its interaction with Mdm2 (refs. 9,10). Nevertheless, biochemical studies show that phosphorylation of the p53 TAD-I is not sufficient to abolish its interaction with Mdm2, suggesting that, *in vivo*, other determinants are required for full p53 activation<sup>11–13</sup>. Providing additional complexity, the central acidic domain of Mdm2 interacts with the DNA-binding domain of p53 (within conserved regions IV and V, residues 234–286), and these contacts are essential for proper p53 ubiquitination<sup>14–16</sup>. Indeed, p53 lacking its TAD-I region is still able to interact with Mdm2 in pulldown experiments and is efficiently ubiquitinated by Mdm2 *in vitro*<sup>17</sup>.

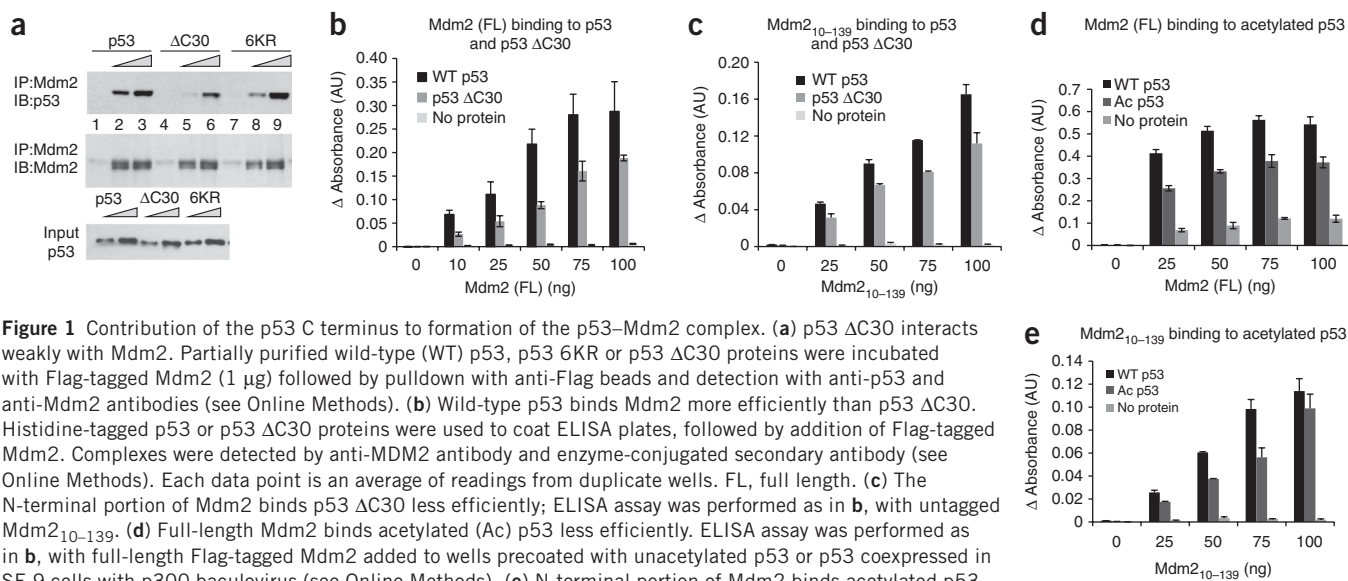
The key lysines of p53 that are ubiquitinated by Mdm2 reside within its extreme C-terminal 30 residues (p53 CTD)<sup>18</sup>. In addition

to ubiquitination, small ubiquitin-like modifier (SUMO), neural precursor cell expressed developmentally downregulated (NEDD8), acetyl groups and methyl groups can also modify the cluster of lysines in the p53 CTD<sup>19</sup>. These modifications are deposited and removed from the ε-NH<sub>3</sub> groups of the lysines by numerous enzymes including the histone acetylase p300, which interacts with the N-terminal domain of p53 (ref. 19). The ability of Mdm2 to stimulate ubiquitination of the p53 CTD while interacting with distal parts of the protein is still poorly understood, as is the exact mechanism by which RING-type E3 ligases facilitate ubiquitination of their targets.

Previous studies have alluded to the physical separation of Mdm2 and p53 following C-terminal ubiquitination of p53 (refs. 20,21). Previous work<sup>21</sup> described monoubiquitination as causal of p53 nuclear export, and other studies<sup>20</sup> expanded on these data to show that Mdm2 dissociates from p53 upon p53 monoubiquitination. This has primarily been shown through changes in the localization of a p53-ubiquitin fusion protein from the nucleus to the cytoplasm, although a more recent report showed dissociation between Mdm2–p53 following p53 acetylation<sup>22</sup>. The authors of the above reports acknowledge that the mechanism connecting modifications of the p53 CTD with the release of Mdm2 from the complex remains unclear. Two possibilities emerge: one is that p53 modifications lead to the loss of p53 tetramerization, revealing the nuclear export signal and facilitating export, and the other is that direct contact between Mdm2 and the p53 CTD exists and is regulated by post-translational modifications. Based on results showing that either ubiquitinated or acetylated p53 is competent to activate transcription of p53 target genes, an activity that requires p53 tetramer formation, we chose to pursue an investigation of the latter hypothesis<sup>22,23</sup>.

<sup>1</sup>Department of Biological Sciences, Columbia University, New York, New York, USA. <sup>2</sup>Department of Structural Biology, University of Pittsburgh Medical School, Pittsburgh, Pennsylvania, USA. <sup>3</sup>Institute of Chemistry, Hebrew University of Jerusalem, Safra Campus, Givat Ram, Jerusalem, Israel. <sup>4</sup>Department of Oncological Sciences, Mount Sinai School of Medicine, New York, New York, USA. Correspondence should be addressed to C.P. (clp3@columbia.edu).

Received 4 August 2009; accepted 3 May 2010; published online 18 July 2010; corrected online 25 July 2010; doi:10.1038/nsmb.1872



Here we present evidence of a direct contact between the C terminus of p53 and the N terminus of Mdm2. Further, we show that the complex between Mdm2 and p53 can be regulated by modifications of the p53 CTD.

## RESULTS

### The C terminus of p53 contributes to the p53-Mdm2 complex

To investigate the role of the p53 CTD in the interaction with Mdm2, we first looked at the ability of wild-type human p53, p53 with the C-terminal 30 residues deleted (p53  $\Delta$ C30) and p53 with the six lysines in the CTD substituted for arginine (p53 6KR) to bind human Mdm2. We expressed these p53 proteins in H1299 stable cell lines (Fig. 1a and Supplementary Fig. 1a) and partially purified them on a heparin column, which allows for the isolation of DNA-binding proteins. Because p53 possesses two nucleic acid-binding domains, one at the CTD, the wild-type protein showed higher affinity for heparin than the p53  $\Delta$ C30 protein, as expected (Supplementary Fig. 1b). We performed pull-down assays with wild-type and variant p53 and Flag-tagged full-length Mdm2 (Fig. 1a). Wild-type p53 bound Mdm2 better than p53  $\Delta$ C30, whereas p53 6KR was only marginally defective. Because of the similar elution profiles from the heparin column of wild-type p53 and p53 6KR (Supplementary Fig. 1b), we believe that they have similar overall modifications and thus bind Mdm2 similarly. This is in contrast to previous observations that p53 6KR has higher affinity for endogenous Mdm2 in cells, which was attributed to the protein's inability to become modified<sup>20</sup>.

We assessed the binding of Mdm2 to histidine-tagged p53 and p53  $\Delta$ C30 purified from bacteria, in an ELISA. We coated ELISA plates with p53 or p53  $\Delta$ C30 (Supplementary Figs. 1c-e) and measured bound Mdm2 (full-length or a truncation corresponding to its N-terminal domain) with an anti-Mdm2 antibody. Mdm2 bound preferentially to the wild-type p53 (Fig. 1b), suggesting that the p53 CTD is needed for full interaction with Mdm2. Notably, we also found that p53  $\Delta$ C30 was partially impaired in binding the N terminus of Mdm2<sub>10-139</sub> (Fig. 1c). Therefore, the N-terminal portion of Mdm2 is sufficient to discriminate between full-length and C-terminally truncated p53. Further, these data indicate the existence of a binding site within the N terminus of Mdm2 for the p53 CTD.

Although the p53 CTD is seldom mutated or deleted in tumors<sup>24</sup>, it is a site for multiple modifications, including lysines acetylated by p300 (ref. 19). We tested whether modifications in p53 CTD decrease binding to Mdm2 using Flag-tagged p53 purified from insect cells that were co-infected with a baculovirus producing p300. p53 coexpressed with p300 is highly acetylated, as shown by a gain of reactivity with a Pan-acetyl antibody and corresponding loss of reactivity with an antibody Pab 421 that recognizes unmodified p53 CTD<sub>372-382</sub> (refs. 25,26) (Supplementary Fig. 2a,b). We found that acetylated p53 was less able to bind full-length Mdm2 or Mdm2<sub>10-139</sub> compared to wild-type p53 (Fig. 1d,e). These results are consistent with a direct interaction between the Mdm2 N terminus and the p53 CTD. It should be noted that, in addition to multiple C-terminal sites, p300 also acetylates p53 at Lys164 in its core domain<sup>22</sup>; however, this residue is not near the region that makes contacts with the acidic domain of Mdm2 (ref. 25), indicating that modification of this site should not contribute to the loss of overall binding.

We further probed the interaction of Mdm2 with acetylated p53 using a Fe<sup>2+</sup>-localized hydroxyl radical footprinting assay (Supplementary Fig. 3). The addition of Mdm2 to acetylated or non-acetylated p53 generated a different pattern of cleavage products, with an exclusive cleavage site in unmodified p53. These data suggest that acetylated and nonacetylated p53 bind Mdm2 differently.

### The C terminus of p53 interacts with Mdm2

To confirm that the p53 CTD directly binds the Mdm2 N terminus, we performed three distinct binding assays. First, we assayed the binding of GST-Mdm2<sub>10-139</sub> to a p53 CTD<sub>367-397</sub> peptide in a native gel (Fig. 2a). The basic p53 CTD peptide (pI  $\approx$  10.0) does not enter the gel under the buffer conditions we used (pH 8.5) (Fig. 2a, lanes 9-11). Strikingly, in the presence of GST-Mdm2<sub>10-139</sub>, we were able to detect markedly enhanced migration of the p53 CTD into the native gel (by immunoblotting with PAb 421), consistent with the formation of a complex. The acidic p53 TAD-I<sub>1-42</sub> peptide transverses the gel too rapidly for retention without Mdm2 but was retained in the gel in the presence of Mdm2 (Fig. 2a, lanes 2 and 6-8). Further, the p53 CTD<sub>367-393</sub> bound Mdm2 even in the presence of p53 TAD-I<sub>1-42</sub> peptide, suggesting that the two regions of p53 bind the N terminus of Mdm2 noncompetitively (Fig. 2a, lanes 6-8). Thus, binding Mdm2

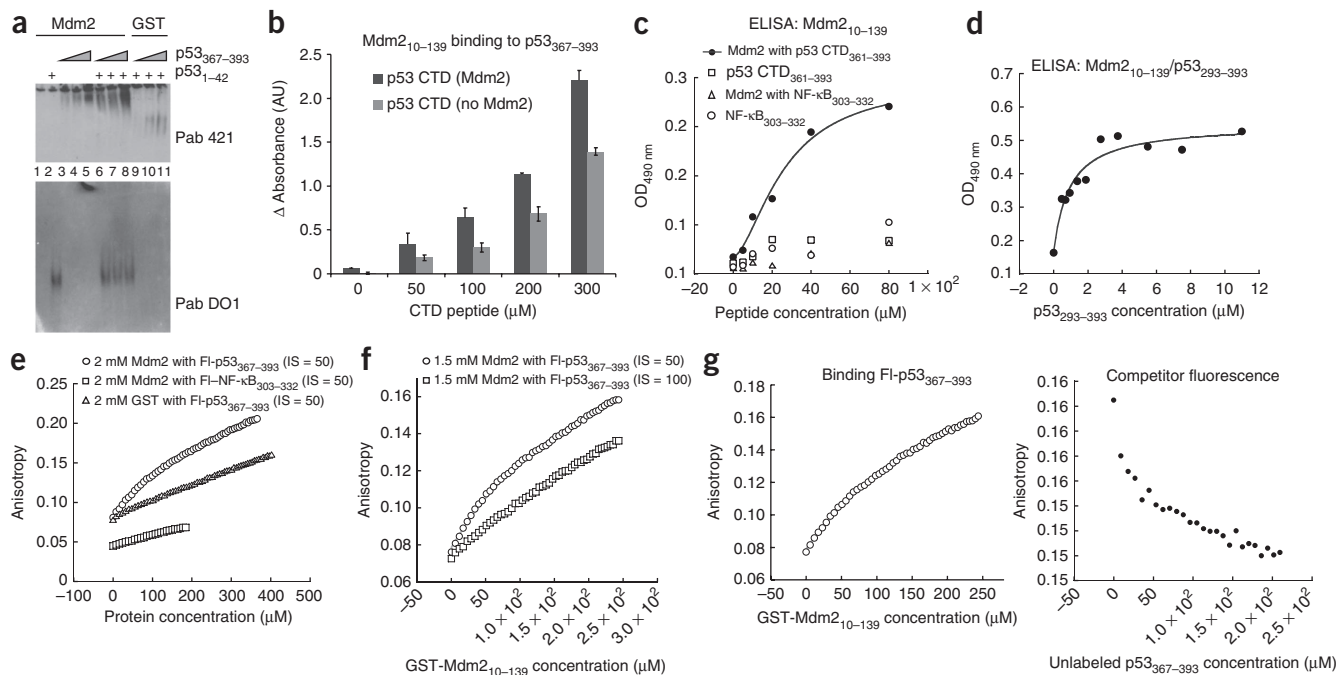


**Figure 2** Analysis of the binding between the N terminus of Mdm2 and p53 CTD. (a) Mdm2 binds p53 CTD in a native gel. We separated 2.5 μg Mdm2<sub>10-139</sub> (lanes 1–8) or GST (lanes 9–11) in complex with p53 TAD-I<sub>1-42</sub> (20 μg) or p53 CTD<sub>367-393</sub> (15, 20 or 40 μg) in a native gel. p53 CTD and p53 TAD-I were visualized by immunoblotting with Pab 421 (top) or Pab DO1 (bottom). (b) p53 CTD binds Mdm2 in an ELISA. Mdm2<sub>10-139</sub> was incubated with increasing concentrations of p53 CTD<sub>367-393</sub>; the bound p53 CTD was detected by Pab 421 (see Online Methods). (c) Histidine (His)-tagged p53 CTD<sub>361-393</sub> binds Mdm2 in an ELISA. Immobilized Mdm2<sub>10-139</sub> was incubated with His-p53 CTD<sub>361-393</sub> or His-NF-κB<sub>303-332</sub> peptides; the bound peptides were detected with anti-His antibody. (d) Mdm2<sub>10-139</sub> binds the longer C-terminal portion of p53 with higher affinity. Immobilized Mdm2<sub>10-139</sub> was incubated with p53<sub>293-393</sub> and the bound fraction of the latter was detected with anti-p53 antibody. (e) GST-Mdm2 binding to a p53 CTD peptide assessed using fluorescence assays. Fluorescein (FI)-labeled peptides (either FI-p53<sub>367-393</sub> or FI-NF-κB<sub>303-332</sub>) were mixed with unlabeled GST or GST-Mdm2<sub>10-139</sub> at indicated concentrations in the buffer containing 50 mM NaCl (IS = 50). (f) Mdm2 interaction with the p53 CTD is electrostatic in nature. Unlabeled GST-Mdm2<sub>10-139</sub> was added to FI-p53<sub>367-393</sub> at indicated NaCl concentrations. (g) Unlabeled p53 CTD peptide competes for binding Mdm2. For fluorescence anisotropy competition experiments, unlabeled p53 CTD<sub>367-393</sub> peptide was titrated into a preformed complex of FI-p53 CTD<sub>367-393</sub> and GST-Mdm2<sub>10-139</sub>. Left, binding curves for complex formation; right, competition.

changes the behavior of the p53 peptides in this assay. Note that, in this assay, neither the CTD nor the TAD peptides appear at the migration position of Mdm2. The fact that the two peptides appear in different positions on the gel is a reflection of their overall charge and not of the binding to two different pools of Mdm2.

Second, we measured the association of a p53 CTD<sub>367-393</sub> peptide with Mdm2<sub>10-139</sub> in a quantitative ELISA (Fig. 2b). We also detected binding of the CTD peptide to full-length Mdm2 in a parallel ELISA (Supplementary Fig. 4). The interpretation of these data, however, is complicated by the potential contribution of nonspecific interaction of the basic CTD peptide with the acidic domain of Mdm2. Additionally, we used a slightly longer histidine-tagged p53<sub>361-393</sub> peptide in the ELISA experiments along with a histidine-tagged NF-κB<sub>303-332</sub> peptide of similar length, which is also very basic (pI ≈ 9.77) (Fig. 2c). The basic NF-κB peptide did not show binding Mdm2 above background. Fitting the curve to a binding equation with a Hill coefficient of ~2, we calculated the  $K_d$  from four independent experiments to be ~30 μM for the binding between the p53 CTD and the N terminus of Mdm2. The addition of the tetramerization domain p53<sub>293-393</sub> markedly improved the binding of p53 to the Mdm2 N terminus in similar ELISA experiments (Fig. 2d). The calculated  $K_d$  was ~1 μM. Note that data in Figure 2d is shown following background subtraction to clearly demonstrate binding saturation. In all, we detected the binding of Mdm2<sub>10-139</sub> and three different versions of the p53 CTD by three different antibodies, revealing a specific interaction with binding affinities in the low micromolar range.

As a third approach, we measured Mdm2 interaction with the p53 CTD using fluorescence anisotropy. We compared the binding of GST alone or of GST-Mdm2<sub>10-139</sub> to the fluorescein-labeled p53<sub>367-393</sub> peptide with the binding of GST-Mdm2<sub>10-139</sub> to a fluorescein-labeled NF-κB<sub>303-332</sub> peptide. Only GST-Mdm2 and fluorescein-labeled p53<sub>367-393</sub> binding produced a rounded curve characteristic of specific binding (Fig. 2e). GST protein, when incubated with increasing amounts of p53 CTD, did not show such a binding curve. Similarly, GST-Mdm2 protein did not show any measurable affinity for the basic fluorescein-labeled NF-κB<sub>303-332</sub> peptide. The inability of GST-Mdm2 to bind the basic NF-κB peptide (pI ≈ 10) is particularly notable because the binding of the p53 CTD with the N terminus of Mdm2 is electrostatic in nature. The affinity of GST-Mdm2 for the p53<sub>367-393</sub> peptide was reduced when we increased the ionic strength of the buffer from 50 to 100 mM NaCl (Fig. 2f). This result implies that the p53 CTD is unlikely to interact with the hydrophobic pocket of Mdm2 and thus would not compete for the binding to the N terminus of Mdm2 with the TAD-I domain of p53. We also used fluorescence anisotropy to confirm that the GST-Mdm2<sub>10-139</sub> and Mdm2<sub>10-139</sub> proteins used in the majority of our biochemical assays are properly folded by measuring their binding to the p53 TAD-I peptide. In both cases, we obtained  $K_d$  values in the nanomolar range, consistent with previously published data (Supplementary Fig. 5).

As an additional specificity control, we performed a competition fluorescence anisotropy experiment. We titrated increasing amounts

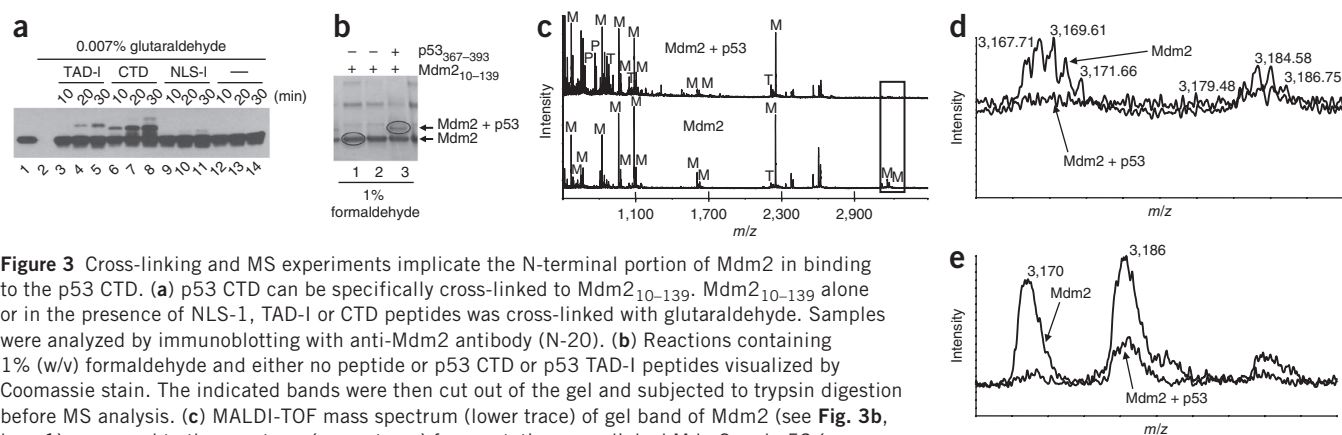


**Figure 3** Cross-linking and MS experiments implicate the N-terminal portion of Mdm2 in binding to the p53 CTD. **(a)** p53 CTD can be specifically cross-linked to Mdm2<sub>10–139</sub>. Mdm2<sub>10–139</sub> alone or in the presence of NLS-1, TAD-I or CTD peptides was cross-linked with glutaraldehyde. Samples were analyzed by immunoblotting with anti-Mdm2 antibody (N-20). **(b)** Reactions containing 1% (w/v) formaldehyde and either no peptide or p53 CTD or p53 TAD-I peptides visualized by Coomassie stain. The indicated bands were then cut out of the gel and subjected to trypsin digestion before MS analysis. **(c)** MALDI-TOF mass spectrum (lower trace) of gel band of Mdm2 (see **Fig. 3b**, lane 1) compared to the spectrum (upper trace) from putative cross-linked Mdm2 and p53 (see **Fig. 3b**, lane 3). Peptide masses identified are labeled as follows: M, Mdm2-derived peptide; P, p53-derived peptide; T, trypsin-derived peptide. **(d)** Overlay of the Mdm2 and Mdm2–p53 spectra suggests that the N-terminal–most part of Mdm2 contacts the p53 CTD. Detail of boxed region in **Figure 3c** showing loss of monoisotopic masses at 3,167.71 and 3,183.70 *m/z* of Mdm2 in the cross-linked samples. **(e)** Using linear method of analysis, the corresponding average masses at 3,170 *m/z*, and 3,186 *m/z* were not completely eliminated, suggesting some tailing in the gel from the main Mdm2 band into the cross-linked Mdm2–p53 band.

of unlabeled p53<sub>367–393</sub> into a preformed complex of GST-Mdm2 and fluorescein-labeled p53<sub>367–393</sub> at an ionic strength of 50 mM NaCl (**Fig. 2g**). The decrease in anisotropy back to the initial values suggests efficient competition.

### Mapping the Mdm2–p53 CTD interaction

We next performed formaldehyde and glutaraldehyde cross-linking experiments as an additional test of binding. Here we subjected 8  $\mu$ M Mdm2<sub>10–139</sub> to glutaraldehyde cross-linking alone or in the presence of 35  $\mu$ M p53 TAD-I, p53 CTD or p53 nuclear localization signal-I (NLS-I) peptides (**Fig. 3a**). Cross-linking resulted in the appearance of novel bands, upshifted by about 5 and 3 kDa in the TAD-I and CTD samples, respectively. The decrease in mobility corresponded to the added molecular weight of the peptide. We also used a p53<sub>305–322</sub> NLS-I peptide that spans a similarly basic region of p53 (pI = 11.3). The intensity of the cross-linked bands corresponds to the probability of cross-link, which is dependent on the number of lysines in each peptide. The p53 TAD-I peptide with only one lysine would cross-link less efficiently than the CTD peptide that has six lysines. However, the fact that p53 TAD-I was cross-linked with much higher efficiency than the p53 NLS-I peptide that contains four lysines serves as a specificity control.

We then performed preparative cross-linking experiments using 1% (w/v) formaldehyde<sup>26</sup>. We excised the bands corresponding to Mdm2 and potentially the Mdm2–p53<sub>367–393</sub> crosslinked heterodimer and subjected them to trypsin digestion and MALDI-TOF analysis (**Fig. 3b**). For the Mdm2-only band (circled in **Fig. 3b**, lane 1), masses of at least 13 peptides were matched by Mascot at 22 p.p.m. r.m.s. deviation (68 peptides were searched) with a Mascot score of 111. For the band with putative Mdm2 and p53 (circled in **Fig. 3b**, lane 3), we detected Mdm2 with a Mascot score of 75 (12 peptides matched out of 96 peptides searched). Masses of 670.34 and 763.41 *m/z* support the presence of peptides WSHLK and KGQSTSR, respectively, from p53 in this gel band (**Fig. 3c**). Furthermore, formaldehyde cross-linking in this band resulted in the loss of a monoisotopic mass (3,167.71 *m/z*) corresponding to peptide GSMTDGAVTTSQIPASEQETLVRPKPLLLK (residues 10–36 of Mdm2) and a monoisotopic peak at 3,183.70 *m/z* corresponding to the same mass with oxidized methionine (**Fig. 3d,e**). The loss of this peptide suggests that it spans a potential site of the interaction between the p53 CTD and Mdm2.

### Mdm2 inhibition of p53 DNA binding requires the p53 C terminus

The p53 CTD has multiple roles in p53 function, serving as a regulatory region and as a non-sequence-specific nucleic acid-interacting domain<sup>27</sup>. If Mdm2 is indeed making contacts with this part of p53, it could also alter the ability of p53 to interact with DNA. To test this hypothesis, we first looked at the binding of heparin-purified p53, p53  $\Delta$ C30 or p53 6KR as well as bacterial p53 and p53  $\Delta$ C30 to a p53 response element from the *p21* promoter in an EMSA. Mdm2 was able to inhibit the p53–DNA interaction in a matter that depended on the presence of the intact CTD (**Fig. 4a,b**). Further, the ability of Mdm2 to inhibit p53–DNA interactions was alleviated by the addition of PAb 421 (**Supplementary Fig. 6**). As we previously showed that the off-rate kinetics of p53 and p53  $\Delta$ C30 are very similar<sup>28</sup>, we believe that the observed changes in p53–DNA association are caused by interaction with Mdm2. In addition to the loss of p53–DNA complex, we detected a small upward shift of the p53 band in the presence of Mdm2, as has been shown previously<sup>22</sup>. The RING domain portion of Mdm2, GST-Mdm2<sub>410–491</sub>, did not affect the p53–DNA interaction, supporting the likelihood that functional contacts are being made in the N-terminal region of Mdm2 (**Fig. 4b**).

To determine whether Mdm2 can affect p53–DNA interactions in cells, we looked at the ability of transfected p53 to interact with the endogenous *p21* promoter in the presence of coexpressed Mdm2 by a chromatin immunoprecipitation (ChIP) assay. Coexpression of p53 with Mdm2 in *p53/Mdm2* doubly null mouse embryonic fibroblasts (2KO) reduced p53 promoter association (**Fig. 4c**, graph), although the levels of p53 were also reduced as a result of the E3 ubiquitin ligase function of Mdm2 (**Fig. 4c**, immunoblot). To coexpress p53 and Mdm2 without p53 degradation, we used an E3-deficient mutant of Mdm2 lacking the last seven residues (Mdm2  $\Delta$ C7)<sup>29</sup>. Mdm2  $\Delta$ C7 did not degrade p53 but was nevertheless able to reduce p53 association with the *p21* promoter (**Fig. 4c**). To establish the role of the p53 CTD in the observed inhibition, we coexpressed p53 or p53  $\Delta$ C30 with Mdm2  $\Delta$ C7. Due to differences in stability between these two proteins, we transfected different amounts of wild-type p53 DNA and p53  $\Delta$ C30 DNA to assure equivalent expression. Reproducing our published data, p53  $\Delta$ C30 was less effective than wild-type p53 at DNA binding in cells<sup>30</sup>. Furthermore, in accord with our *in vitro* DNA binding data, Mdm2 did not affect p53  $\Delta$ C30 binding to the *p21* promoter (**Fig. 4d**). These data suggest that the interaction of

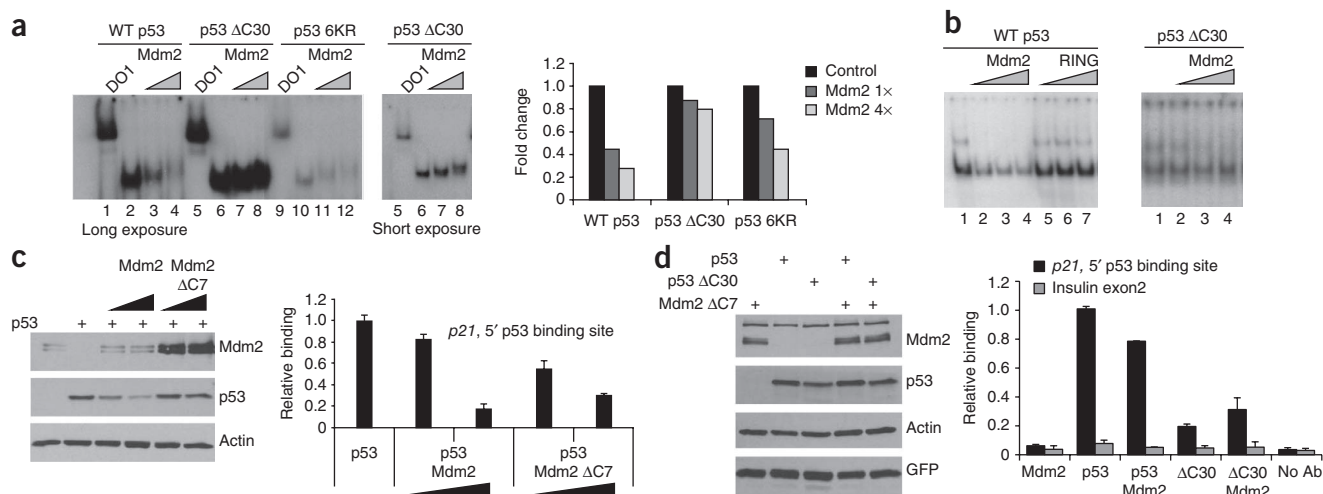


**Figure 4** The p53 C terminus is required for Mdm2 to inhibit p53 DNA binding *in vitro* and in cells. **(a)** Deletion of the C terminus of p53 largely alleviates the ability of Mdm2 to inhibit the p53–DNA interaction. Left, EMSA performed with heparin-purified p53, p53  $\Delta$ C30 and p53 6KR proteins. p53 bound to a 44–base pair fragment spanning the 5' p53 binding site from the *p21* promoter in the presence of Mdm2 (0.5 or 1.0  $\mu$ g). Right, graph representing data in left panel. **(b)** Mdm2 RING domain does not inhibit p53–DNA interaction. EMSA was performed as in **a**. p53 (left) or p53  $\Delta$ C30 (right) (250 ng) bound DNA in the presence of Flag-tagged Mdm2 (0.5, 1.0 or 1.5  $\mu$ g) or GST-Mdm2<sub>410–491</sub> (RING) (0.5, 1.0 or 1.5  $\mu$ g). **(c)** Mdm2  $\Delta$ C7 impairs p53 association with *p21* promoter in cells without lowering p53 protein levels. 2KO mouse cells (*p53*<sup>-/-</sup>; *Mdm2*<sup>-/-</sup>) transfected with Mdm2 or Mdm2  $\Delta$ C7 (10 and 20  $\mu$ g) and p53 (4  $\mu$ g). Protein expression was determined by immunoblotting with anti-Mdm2 (Smp14, 3G5 and 2A10), anti-p53 (PAb 1801 and DO1) and anti-actin antibodies (top three panels). Chromatin samples were amplified by Q-PCR for the 5'–p53 binding site within the *p21* promoter. **(d)** Mdm2  $\Delta$ C7 reduces the association of p53 with the *p21* promoter. 2KO cells were transfected with plasmids expressing Mdm2  $\Delta$ C7 (10  $\mu$ g), p53 (4  $\mu$ g), p53  $\Delta$ C30 (0.4  $\mu$ g) and GFP (0.1  $\mu$ g). Extracts were analyzed as in **c** and *insulin* exon2 was used as a negative control. Ab, antibody.

the p53 C terminus with Mdm2 can have functional consequences that extend beyond facilitating its ubiquitination by Mdm2.

#### Nutlin-3 and TAD-I region of p53 bind Mdm2 N terminus differently

Because multiple contacts contribute to the Mdm2–p53 complex, we wanted to determine the relative contributions of the Mdm2 acidic domain and the p53 CTD to the overall binding. To this end, we tested the ability of Mdm2 and p53 to interact in the presence of Nutlin-3 or p53 TAD-I<sub>1–42</sub>. Both of these reagents have been reported to have nanomolar affinities for Mdm2 and to effectively block complex formation between Mdm2<sub>25–128</sub> and p53<sub>1–312</sub> (refs. 6,31). Accordingly, Nutlin-3 completely blocked the interaction between Mdm2<sub>10–139</sub> and

the p53 TAD-I<sub>1–42</sub> peptide in native gel experiments (**Supplementary Fig. 7**). In ELISA-dissociation experiments, however, both Nutlin-3 and p53 TAD-I<sub>1–42</sub> peptide inhibited binding between full-length p53 and Mdm2<sub>10–139</sub> with IC<sub>50</sub> values of  $\sim$ 1  $\mu$ M (**Fig. 5a**). Because earlier reported competition studies were performed with p53 lacking its C terminus, we believe that the difference in affinity we observed (nM versus  $\mu$ M IC<sub>50</sub> values) is due to the contribution of the contacts made by the p53 CTD to the Mdm2–p53 complex. Indeed, when testing the ability of Nutlin-3 and the p53 TAD-I<sub>1–42</sub> peptide to block the binding of full-length p53 and full-length Mdm2, we observed that the IC<sub>50</sub> for Nutlin-3 was  $\sim$ 10  $\mu$ M, whereas the TAD-I peptide showed very limited inhibition of the interaction (**Fig. 5b**). Based on

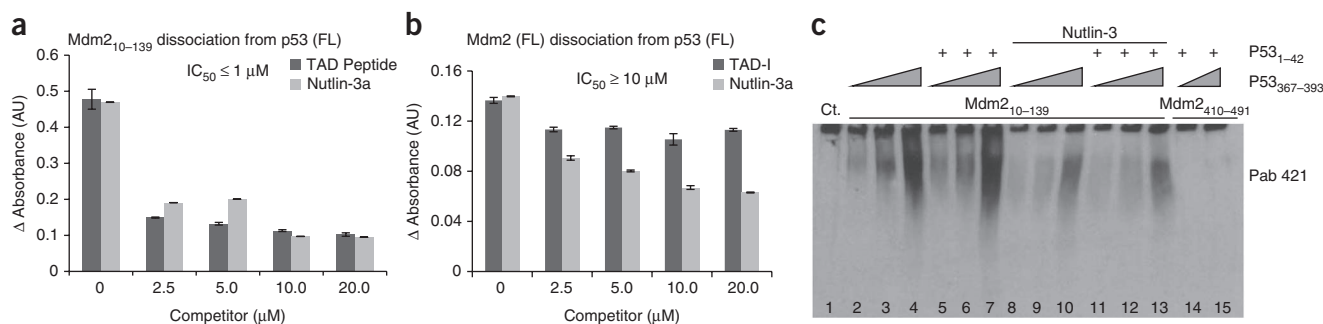
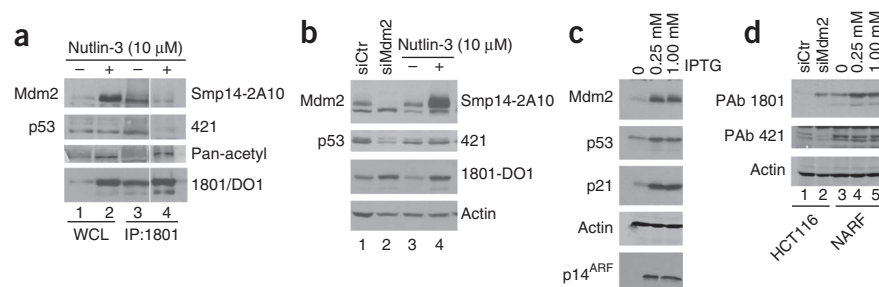


**Figure 5** Nutlin-3 inhibits Mdm2–p53 complex formation and leads to modification of the p53 C terminus. **(a)** Nutlin-3 and a p53 N-terminal peptide (TAD-I) each disrupt the interaction of p53 with the N terminus of Mdm2. ELISA was carried out as described in **Figure 1c**; hexahistidine-tagged p53 (100 ng) and untagged Mdm2<sub>10–139</sub> (70 ng) were added to the p53-coated wells alone or in the presence of increasing amounts of Nutlin-3 or TAD-I<sub>1–42</sub>. Bound Mdm2 was measured by anti-Mdm2 N-20 reactivity. FL, full length. **(b)** Neither Nutlin-3 nor a p53 TAD-I peptide can completely disrupt the interactions between full-length Mdm2 and full-length p53. ELISA was carried out as in **a**. Flag-tagged Mdm2 (100 ng) was added to each well alone or in the presence of Nutlin-3 or TAD-I<sub>1–42</sub> peptide, and bound Mdm2 was determined by reactivity with N-20 antibody. **(c)** Nutlin-3 reduces binding of the p53 CTD to the N terminus of Mdm2. Reaction mixtures with 450 ng GST-Mdm2<sub>10–139</sub> (lanes 2–13) or GST-Mdm2<sub>410–491</sub> (lanes 14 and 15) contained increasing amounts of p53<sub>367–393</sub> (40, 80, 160  $\mu$ M) and p53<sub>1–42</sub> (25  $\mu$ M) where indicated. Additionally, mixtures in lanes 8–13 included 25  $\mu$ M Nutlin-3, dissolved in DMSO. The final volume of DMSO in all reaction mixtures was 10% (v/v).

**Figure 6** Nutlin-3, p14<sup>ARF</sup> and Mdm2 siRNA induce C-terminal modifications of p53.

(a) HCT116 cells were treated in parallel with DMSO or Nutlin-3 (10  $\mu$ M) for 4 h. Soluble extracts (75  $\mu$ g; WCL) were subjected to immunoblotting with the antibodies indicated at right. p53 was immunoprecipitated with PAb 1801 from 1 mg of the same extracts (IP:1801). Lane 3 contained 5 $\times$  volume of immunoprecipitated sample loaded in lane 4, to attempt to normalize for the amount of p53 on the gel. For p53 detection, the blot was

probed with PAb 421, stripped and reprobred with PAb 1801-DO1 mixture, then stripped again and reprobred with the Pan-acetyl antibody. (b) HCT116 cells, treated with Nutlin-3 (lanes 3 and 4) as in **a** or transiently transfected for 72 h with either control or Mdm2 siRNA (siCtr and siMdm2, respectively; lanes 1 and 2). p53 was first detected by PAb 421, stripped and reprobred with PAb 1801-DO1 mixture. (c) U2OS cells stably expressing p14<sup>ARF</sup> under the control of IPTG (NARF) were grown exponentially, and p14<sup>ARF</sup> was induced for 24 h. Following treatment, lysates (75  $\mu$ g) were resolved by SDS-PAGE and subjected to immunoblotting with the indicated antibodies. (d) We resolved 75  $\mu$ g of soluble extracts from HCT116 cells treated with siMdm2 (lanes 1 and 2) as well as NARF cells induced by IPTG (lanes 3–5) by SDS-PAGE and subjected them to immunoblotting with the indicated antibodies. For p53 detection, the blot was first probed with PAb 421, stripped and reprobred with PAb 1801-DO1 mixture.



these data, we postulate that, *in vitro*, both the core domain of p53 and the p53 CTD make appreciable energetic contributions to the overall complex. This implies that, even when the interaction between the N termini of these proteins is disrupted, additional modification of the acidic domain of Mdm2 and/or the CTD of p53 may be necessary to completely dissociate Mdm2 and p53 *in vivo*.

We tested at the ability of the p53 CTD<sub>367–393</sub> peptide to interact with Mdm2<sub>10–139</sub> in a native gel alone or in the presence of Nutlin-3 or the p53 TAD-I<sub>1–42</sub> peptide. The addition of the TAD-I<sub>1–42</sub> peptide did not disrupt the p53 CTD<sub>367–393</sub> interaction with Mdm2. Nevertheless, Nutlin-3 reduced the binding between the CTD and Mdm2 in this assay (Fig. 5c). These data fall in line with an NMR investigation that compared the structures of the Mdm2 N-terminal domain alone, bound to p53 or bound to Nutlin-3 and showed that Nutlin-3 binds Mdm2 via a mechanism distinct from that of p53 (ref. 32). Thus, it is possible that Nutlin-3-induced changes, which are perhaps refractory to CTD binding, are further contributing to the *in vivo* efficacy of this compound.

### Nutlin-3 and p14<sup>ARF</sup> induce modification of the p53 CTD

Having accumulated a substantial amount of data showing the interaction between the p53 CTD and the N terminus of Mdm2, we were faced with a contradictory issue. *In vivo*, inhibitors of the binding between the N terminus of p53 and the N terminus of Mdm2 (such as Nutlin-3) are able to effectively stabilize p53 and activate p53 function<sup>8,33–37</sup>. Nutlin-3 was reported to cause p53 stabilization without p53 being phosphorylated at several known stress-inducible sites<sup>38</sup>. If Nutlin-3 was able to completely inhibit p53–Mdm2 complex formation without induction of any p53 post-translational modifications, then our *in vitro* binding data would not be relevant under physiological conditions. However, if the dissociation of the N-terminal binding domains leads to increased C-terminal modifications (such as acetylation) of p53 *in vivo*, it is possible that Nutlin-3 treatment would not only affect the N-terminal interaction but would also decrease the C-terminal interaction as well.

We treated HCT116 cells with 10  $\mu$ M Nutlin-3 and, as expected, levels of p53 and Mdm2 increased when detected in whole-cell extracts with a mixture of p53 N-terminal antibodies (PAb 1801 and DO1) and Mdm2 antibodies (SMP14 and 2A10), respectively (Fig. 6a, left, lanes 1 and 2, and right, lanes 3 and 4). Consistent with the proposed mechanism of action of Nutlin-3, p53 in cells treated with this compound was not able to interact with Mdm2, as we were only able to detect Mdm2 in p53 immunoprecipitates from untreated cells (Fig. 6a, lanes 3 and 4).

Strikingly, when we detected p53 in these cells with modification-sensitive PAb 421, there was no increase in reactivity after Nutlin-3 treatment (Fig. 6a, lanes 1 and 2, and Fig. 6b, lanes 3 and 4). Ablating Mdm2 by siRNA in these cells also caused an overall p53 accumulation and a decrease in 421-detectable p53, confirming the validity of using PAb 421 reactivity as readout of p53 CTD modifications (Fig. 6b, lanes 1 and 2). This result correlates with our earlier finding that having excess Mdm2 in cells leads to a decrease in p53 C-terminal acetylation<sup>39</sup>. Using a Pan-acetyl antibody, we saw an increase in signal from p53 after treatment (Fig. 6a). Thus, Nutlin-3 induces modifications of p53 at the C terminus (including acetylation), and this likely diminishes the interaction of the p53 CTD with Mdm2.

It has been previously reported that p14<sup>ARF</sup> expression is able to stabilize p53 in the absence of N-terminal modifications<sup>40</sup>. To test the effects of p14<sup>ARF</sup> on the p53 CTD modifications, we used NARF cells<sup>41</sup>. p14<sup>ARF</sup> induction led to stabilization of p53 and accumulation of p21 and Mdm2 (Fig. 6c). We then compared PAb 421 and PAb 1801-DO1 reactivity of p53 in NARF cells. Similarly to Nutlin-3 treatment, the amount of p53 detected by a mixture of PAb 1801-DO1 antibodies increased following p14<sup>ARF</sup> induction, whereas PAb 421 reactivity remained unchanged (Fig. 6d, lanes 3–5). Thus, three distinct DNA damage-independent Mdm2 inhibitors were able to stimulate modifications of p53 CTD, most likely by shifting binding equilibrium away from Mdm2 and toward other modifying enzymes.

### DISCUSSION

The interaction of Mdm2 and p53 is a highly regulated fine-tuned process. Here we describe an additional level of modulation of this association. Using different approaches, we show that the p53 CTD interacts directly with the Mdm2 N terminus. C-terminal modifications of p53 can contribute to the full dissociation of Mdm2–p53 complex *in vivo*, and Nutlin-3 treatment or p14<sup>ARF</sup> overexpression can induce C-terminal modifications of p53 in cells. We propose a model where multiple interactions between p53 and MDM2 act in concert for optimal regulation of p53 (Fig. 7).

We calculated the binding constant for the Mdm2–p53 CTD complex to be in the low micromolar range, which is similar to the affinity of peptides from the Mdm2 acidic region for p53 core domain (in the range of 10–100  $\mu$ M (refs. 14–16)) but much weaker than the interaction of Mdm2 with the p53 N terminus (nanomolar range). Although we were unable to obtain evidence for complex formation by NMR (Supplementary Fig. 8), multiple other assays confirmed direct binding, and our data indicate that p53 CTD–Mdm2 interaction

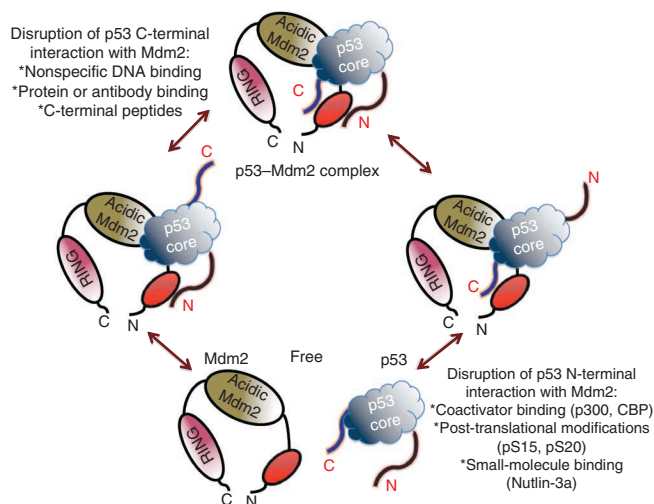


**Figure 7** Proposed mechanism for the function of the p53 C terminus and its modifications in Mdm2 complex formation. Model postulates interactions between three p53 and three Mdm2 regions. Within the N-terminal ~140 residues of Mdm2 are predicted to be two discrete surfaces that interact with the N and C termini of p53, respectively; the third interacting surfaces are within the central regions of p53 (core domain) and Mdm2 (the acidic region). Modifications at the N terminus of p53 or disruption of its contacts with Mdm2 *in vivo* facilitate further modifications at the C terminus, leading to full disruption of the complex. Alternatively, modification(s) within the C terminus of p53 could destabilize the Mdm2–p53 complex, favoring its dissociation.

is important for overall Mdm2–p53 binding. Indeed, the rather low affinity of the CTD for Mdm2 may actually be essential to allow this interaction to be modulated by modifications of the lysines in this region of the protein.

The interaction between the p53 CTD and Mdm2 described here provides a potential mechanism for published observations linking C-terminal modifications of p53 and the dissociation of the Mdm2–p53 complex<sup>20,22</sup>. We have only addressed the effects of C-terminal acetylation of p53 on the Mdm2–p53 complex formation; the global regulatory scheme is likely to be far more complex. Mdm2 is extensively phosphorylated within its acidic domain<sup>19,42,43</sup>. The interaction of the Mdm2 acidic domain with the box IV and box V regions of p53 is essential for proper p53 ubiquitination by Mdm2 (ref. 14). Our results that the Mdm2–p53 complex involves multiple contacts are consistent with the observations that the Nutlin-3 and TAD-I peptides or the removal of the 116 N-terminal residues of p53 do not block the ability of Mdm2 to ubiquitinate p53 *in vitro*<sup>15,17</sup>. It would be exciting to investigate effects of posttranslational modifications of Mdm2 and p53 from the perspective of their ability to stimulate or inhibit the formation of the multiple Mdm2/p53 interfaces.

The data (see **Figs. 2a** and **5c**) showing that the binding of p53 CTD and TAD-I domains to Mdm2 are not mutually exclusive presuppose that different surfaces within the Mdm2 N terminus contact the TAD-I and p53 CTD. Indeed, our preliminary MALDI-TOF analysis suggests that the p53 CTD interacts with the flexible lid region at the N terminus of Mdm2. This is of considerable interest, as apo Mdm2 predominantly exists in the closed conformation, which disfavors p53 interaction<sup>32,44</sup>. Potentially, binding of the basic p53 CTD to this region would disrupt the intramolecular contacts made by the lid region and facilitate the conversion of Mdm2 to an open conformation, thereby stimulating the binding of the TAD-I

domain. Our findings also predict that the N and C termini of p53 are in spatial proximity, at least while both are bound to Mdm2. The putative closeness of the N and C termini of p53 in the context of the intact p53 tetramer could provide additional mechanisms of p53 regulation and could facilitate Mdm2-mediated ubiquitination of this region. Perhaps modifications of the p53 CTD disrupt contacts not only with Mdm2 but alter the spatial relationship between the TAD-I and the p53 CTD, causing long-range conformational changes in the overall protein structure. Such changes could contribute to the loss of Mdm2 binding and could have other functional consequences for p53-mediated transcription.

Nutlin-3 activates p53 efficiently *in vivo*. Based on our data, we propose that multiple cooperating factors are needed for a robust p53 response. According to our model, Nutlin-3 disrupts the N terminus of p53 from binding Mdm2, thus freeing the p53 N terminus to bind other C-terminal modifiers such as p300 (refs. 45,46). Consequent modifications of the p53 C terminus further destabilize the Mdm2–p53 complex. Thus, Nutlin-3 treatment shifts the competition between positive and negative regulators of p53 toward the positive regulators<sup>19,47</sup> (**Fig. 7**). Both Nutlin-3 treatment and p14<sup>ARF</sup> expression lead to accumulation of p53 protein that lacks DNA damage–inducible phosphorylation marks at multiple N-terminal sites<sup>38,40</sup>. In this light, the induction of C-terminal modifications by both of these pathways seems highly noteworthy, as such modifications could dictate differential transcriptional programs and could lead to varying outcomes depending on cellular context. It has been reported that phosphorylation of p53 at key N-terminal residues induces association with p300, leading to C-terminal modification<sup>48,49</sup>. However, unphosphorylated p53 is still able to bind p300, and we believe that this interaction would be favored in cells where Mdm2 is either sequestered in complex with p14<sup>ARF</sup> or inhibited by Nutlin-3. Additionally, it is possible that Nutlin-3 and other p53-activating compounds are more effective in cancer cells<sup>6,8</sup>—these cells may already have a low level of stress-induced modifications on p53 (refs. 50,51), so the dissociation of Mdm2 and p53 would be accomplished more easily in such cells.

Finally, our finding of a third interface between p53 and Mdm2 allows for a more detailed view of the complex and could provide additional avenues for therapeutic activation of wild-type p53 in cells.

## METHODS

Methods and any associated references are available in the online version of the paper at <http://www.nature.com/nsmb/>.

*Note: Supplementary information is available on the Nature Structural & Molecular Biology website.*

## ACKNOWLEDGMENTS

We are exceedingly grateful to E. Freulich for her expert technical assistance and members of the Prives laboratory for their helpful suggestions. This work was supported by grant CA58316 from the US National Institutes of Health to C.P. A.F. is supported by a starting grant from the European Research Council under the European Community's Seventh Framework Programme (FP7/2007–2013)/ERC Grant agreement n°203413.

## AUTHOR CONTRIBUTIONS

M.V.P., A.F. and C.P. designed research; M.V.P., C.K., O.L., M.L., J.A., I.-J.L.B., R.G., M.M., A.Z. and L.M.B. performed research and analyzed data; M.V.P. and C.P. wrote the manuscript.

## COMPETING FINANCIAL INTERESTS

The authors declare no competing financial interests.

Published online at <http://www.nature.com/nsmb/>.

Reprints and permissions information is available online at <http://npg.nature.com/reprintsandpermissions/>.

1. Vousden, K.H. & Prives, C. Blinded by the light: the growing complexity of p53. *Cell* **137**, 413–431 (2009).
2. Barak, Y., Gottlieb, E., Juven-Gershon, T. & Oren, M. Regulation of mdm2 expression by p53: alternative promoters produce transcripts with nonidentical translation potential. *Genes Dev.* **8**, 1739–1749 (1994).
3. Haupt, Y., Maya, R., Kazaz, A. & Oren, M. Mdm2 promotes the rapid degradation of p53. *Nature* **387**, 296–299 (1997).
4. Lin, J., Chen, J., Elenbaas, B. & Levine, A.J. Several hydrophobic amino acids in the p53 amino-terminal domain are required for transcriptional activation, binding to mdm-2 and the adenovirus 5 E1B 55-kD protein. *Genes Dev.* **8**, 1235–1246 (1994).
5. Kussie, P.H. *et al.* Structure of the MDM2 oncoprotein bound to the p53 tumor suppressor transactivation domain. *Science* **274**, 948–953 (1996).
6. Vassilev, L.T. *et al.* *In vivo* activation of the p53 pathway by small-molecule antagonists of MDM2. *Science* **303**, 844–848 (2004).
7. Klein, C. & Vassilev, L.T. Targeting the p53–MDM2 interaction to treat cancer. *Br. J. Cancer* **91**, 1415–1419 (2004).
8. Issaeva, N. *et al.* Small molecule RITA binds to p53, blocks p53–HDM-2 interaction and activates p53 function in tumors. *Nat. Med.* **10**, 1321–1328 (2004).
9. Shieh, S.Y., Ikeda, M., Taya, Y. & Prives, C. DNA damage-induced phosphorylation of p53 alleviates inhibition by MDM2. *Cell* **91**, 325–334 (1997).
10. Appella, E. & Anderson, C.W. Signaling to p53: breaking the posttranslational modification code. *Pathol. Biol. (Paris)* **48**, 227–245 (2000).
11. Kane, S.A. *et al.* Development of a binding assay for p53/HDM2 by using homogeneous time-resolved fluorescence. *Anal. Biochem.* **278**, 29–38 (2000).
12. Sakaguchi, K. *et al.* Damage-mediated phosphorylation of human p53 threonine 18 through a cascade mediated by a casein 1-like kinase. Effect on Mdm2 binding. *J. Biol. Chem.* **275**, 9278–9283 (2000).
13. Lai, Z., Auger, K.R., Manubay, C.M. & Copeland, R.A. Thermodynamics of p53 binding to hdm2(1–126): effects of phosphorylation and p53 peptide length. *Arch. Biochem. Biophys.* **381**, 278–284 (2000).
14. Shimizu, H. *et al.* The conformationally flexible S9–S10 linker region in the core domain of p53 contains a novel MDM2 binding site whose mutation increases ubiquitination of p53 *in vivo*. *J. Biol. Chem.* **277**, 28446–28458 (2002).
15. Wallace, M., Worrall, E., Pettersson, S., Hupp, T.R. & Ball, K.L. Dual-site regulation of MDM2 E3-ubiquitin ligase activity. *Mol. Cell* **23**, 251–263 (2006).
16. Yu, G.W. *et al.* The central region of HDM2 provides a second binding site for p53. *Proc. Natl. Acad. Sci. USA* **103**, 1227–1232 (2006).
17. Ma, J. *et al.* A second p53 binding site in the central domain of Mdm2 is essential for p53 ubiquitination. *Biochemistry* **45**, 9238–9245 (2006).
18. Rodriguez, M.S., Desterro, J.M., Lain, S., Lane, D.P. & Hay, R.T. Multiple C-terminal lysine residues target p53 for ubiquitin-proteasome-mediated degradation. *Mol. Cell. Biol.* **20**, 8458–8467 (2000).
19. Carter, S. & Vousden, K.H. Modifications of p53: competing for the lysines. *Curr. Opin. Genet. Dev.* **19**, 18–24 (2009).
20. Carter, S., Bischof, O., Dejean, A. & Vousden, K.H. C-terminal modifications regulate MDM2 dissociation and nuclear export of p53. *Nat. Cell Biol.* **9**, 428–435 (2007).
21. Li, M. *et al.* Mono- versus polyubiquitination: differential control of p53 fate by Mdm2. *Science* **302**, 1972–1975 (2003).
22. Tang, Y., Zhao, W., Chen, Y., Zhao, Y. & Gu, W. Acetylation is indispensable for p53 activation. *Cell* **133**, 612–626 (2008).
23. Le Cam, L. *et al.* E4F1 is an atypical ubiquitin ligase that modulates p53 effector functions independently of degradation. *Cell* **127**, 775–788 (2006).
24. Hainaut, P. *et al.* IARC Database of p53 gene mutations in human tumors and cell lines: updated compilation, revised formats and new visualisation tools. *Nucleic Acids Res.* **26**, 205–213 (1998).
25. Cho, Y., Gorina, S., Jeffrey, P.D. & Pavletich, N.P. Crystal structure of a p53 tumor suppressor-DNA complex: understanding tumorigenic mutations. *Science* **265**, 346–355 (1994).
26. Sutherland, B.W., Toews, J. & Kast, J. Utility of formaldehyde cross-linking and mass spectrometry in the study of protein-protein interactions. *J. Mass Spectrom.* **43**, 699–715 (2008).
27. Ahn, J. & Prives, C. The C-terminus of p53: the more you learn the less you know. *Nat. Struct. Biol.* **8**, 730–732 (2001).
28. Cain, C., Miller, S., Ahn, J. & Prives, C. The N terminus of p53 regulates its dissociation from DNA. *J. Biol. Chem.* **275**, 39944–39953 (2000).
29. Poyurovsky, M.V. *et al.* The Mdm2 RING domain C-terminus is required for supramolecular assembly and ubiquitin ligase activity. *EMBO J.* **26**, 90–101 (2007).
30. McKinney, K., Mattia, M., Gottifredi, V. & Prives, C. p53 linear diffusion along DNA requires its C terminus. *Mol. Cell* **16**, 413–424 (2004).
31. Schon, O., Friedler, A., Bycroft, M., Freund, S.M. & Fersht, A.R. Molecular mechanism of the interaction between MDM2 and p53. *J. Mol. Biol.* **323**, 491–501 (2002).
32. Showalter, S.A., Bruschiweiler-Li, L., Johnson, E., Zhang, F. & Bruschiweiler, R. Quantitative lid dynamics of MDM2 reveals differential ligand binding modes of the p53-binding cleft. *J. Am. Chem. Soc.* **130**, 6472–6478 (2008).
33. Ding, K. *et al.* Structure-based design of potent non-peptide MDM2 inhibitors. *J. Am. Chem. Soc.* **127**, 10130–10131 (2005).
34. Garcia-Echeverria, C., Chene, P., Blommers, M.J. & Furet, P. Discovery of potent antagonists of the interaction between human double minute 2 and tumor suppressor p53. *J. Med. Chem.* **43**, 3205–3208 (2000).
35. Duncan, S.J., Cooper, M.A. & Williams, D.H. Binding of an inhibitor of the p53/MDM2 interaction to MDM2. *Chem. Commun. (Camb.)* 316–317 (2003).
36. Bottger, V. *et al.* Identification of novel mdm2 binding peptides by phage display. *Oncogene* **13**, 2141–2147 (1996).
37. Vassilev, L.T. Small-molecule antagonists of p53–MDM2 binding: research tools and potential therapeutics. *Cell Cycle* **3**, 419–421 (2004).
38. Thompson, T. *et al.* Phosphorylation of p53 on key serines is dispensable for transcriptional activation and apoptosis. *J. Biol. Chem.* **279**, 53015–53022 (2004).
39. Ohkubo, S., Tanaka, T., Taya, Y., Kitazato, K. & Prives, C. Excess HDM2 impacts cell cycle and apoptosis and has a selective effect on p53-dependent transcription. *J. Biol. Chem.* **281**, 16943–16950 (2006).
40. de Stanchina, E. *et al.* E1A signaling to p53 involves the p19(ARF) tumor suppressor. *Genes Dev.* **12**, 2434–2442 (1998).
41. Stott, F.J. *et al.* The alternative product from the human CDKN2A locus, p14(ARF), participates in a regulatory feedback loop with p53 and MDM2. *EMBO J.* **17**, 5001–5014 (1998).
42. Hay, T.J. & Meek, D.W. Multiple sites of *in vivo* phosphorylation in the MDM2 oncoprotein cluster within two important functional domains. *FEBS Lett.* **478**, 183–186 (2000).
43. Blattner, C., Hay, T., Meek, D.W. & Lane, D.P. Hypophosphorylation of Mdm2 augments p53 stability. *Mol. Cell. Biol.* **22**, 6170–6182 (2002).
44. McCoy, M.A., Gesell, J.J., Senior, M.M. & Wyss, D.F. Flexible lid to the p53-binding domain of human Mdm2: implications for p53 regulation. *Proc. Natl. Acad. Sci. USA* **100**, 1645–1648 (2003).
45. Ito, A. *et al.* p300/CBP-mediated p53 acetylation is commonly induced by p53-activating agents and inhibited by MDM2. *EMBO J.* **20**, 1331–1340 (2001).
46. Kobet, E., Zeng, X., Zhu, Y., Keller, D. & Lu, H. MDM2 inhibits p300-mediated p53 acetylation and activation by forming a ternary complex with the two proteins. *Proc. Natl. Acad. Sci. USA* **97**, 12547–12552 (2000).
47. Wahl, G.M. Mouse bites dogma: how mouse models are changing our views of how P53 is regulated *in vivo*. *Cell Death Differ.* **13**, 973–983 (2006).
48. Feng, H. *et al.* Structural basis for p300 Taz2-p53 TAD1 binding and modulation by phosphorylation. *Structure* **17**, 202–210 (2009).
49. Jenkins, L.M. *et al.* Two distinct motifs within the p53 transactivation domain bind to the Taz2 domain of p300 and are differentially affected by phosphorylation. *Biochemistry* **48**, 1244–1255 (2009).
50. Gorgoulis, V.G. *et al.* Activation of the DNA damage checkpoint and genomic instability in human precancerous lesions. *Nature* **434**, 907–913 (2005).
51. Bartkova, J. *et al.* DNA damage response as a candidate anti-cancer barrier in early human tumorigenesis. *Nature* **434**, 864–870 (2005).

## ONLINE METHODS

**Plasmids and antibodies.** Plasmids encoding human Mdm2, Mdm2  $\Delta$ C7, GST-Mdm2<sub>410–491</sub> and GST-Mdm2<sub>10–139</sub> were previously described<sup>29</sup>. The HA-p53 and p53  $\Delta$ C30 were cloned for mammalian expression from the CMV promoter in PcDNA-3 vector. Mdm2 proteins were detected with hybridoma supernatants (SMP14, 2A10, 3G5) or polyclonal antibody N20 (SantaCruz). p53 proteins were detected with hybridoma supernatants (Pab 1801, DO1 and 421) as indicated. Pan-acetyl antibody was purchased from Cell Signaling. p53 in ELISA experiments was detected with either purified PAb 421, rabbit polyclonal p53 FL-393 (SantaCruz) or histidine probe-conjugated HRP (SantaCruz) antibodies as indicated.

**Electrophoretic mobility shift assay.** EMSA experiments were performed as previously described<sup>52</sup>.

**Enzyme-linked immunosorbent assay.** ELISA experiments were performed as previously described<sup>53</sup>. Briefly, proteins in 200  $\mu$ l of phosphate-buffered saline (PBS) were used to coat wells in a 96-well Pro-bind plate (Falcon) at 4 °C overnight (16 h). The wells were then washed three times in PBS containing 0.05% (v/v) Tween and then incubated in blocking buffer (PBS containing 0.05% Tween and 1% (w/v) bovine serum albumin) for 1 h at 4 °C. Increasing amounts of binding protein (as indicated) were added to the wells in PBS for 2 h at 4 °C. The wells were washed three times with PBS containing 0.05% (v/v) Tween, at which time binding protein-specific antibody in blocking buffer was added and incubated for 1 h at room temperature (23 °C). After three washes, a 1:2,000 dilution of monoclonal anti-rabbit or anti-mouse IgG antibody conjugated to alkaline phosphatase (Sigma) in blocking buffer was added and incubated at room temperature (23 °C) for 30 min. After five washes, 10 mM *p*-nitrophenol phosphate (Sigma) in 100 mM 2-amino-2-methyl-1,3-propanediol (Sigma) was added to the wells. Absorbance at 490 nm was measured at 1-min intervals using a Victor3 Plate Reader (PerkinElmer).

**Fluorescence spectrometry.** Titration of Mdm2 into the fluorescein-labeled peptides was performed in 20 mM HEPES at pH 7.3 with ionic strength of 50 mM or 100 mM. Fluorescence was measured with excitation at 480 nm and emission at 530 nm. The bandwidths were changed depending on the amount of the labeled molecule used. The labeled peptide was placed in the cuvette in a volume of 1 ml, at a concentration of 100 nM, and 100–200  $\mu$ l of GST-Mdm2 or GST (1.4–2 mM) were placed in the dispenser. Additions of 4  $\mu$ l were titrated at 1-min intervals, the solution was stirred for 10 s and the fluorescence and anisotropy were measured. The data were fit to a 1:1 binding model<sup>54</sup>. In the competition binding assay, the conditions were as follows: 100  $\mu$ l of unlabeled p53<sub>367–393</sub> (2,724 nM) were added to a 1,200- $\mu$ l mixture of 100 nM fluorescein-labeled p53<sub>367–393</sub> and 1.4 mM GST-Mdm2 at ionic strength of 50 mM. Measurements were performed as previously described<sup>54</sup>.

**Native gel experiments.** 4% acrylamide-Tris/borate gels without SDS were run at pH 8.5 in 1 $\times$  TB running buffer (90 mM Tris, 90 mM boric acid). Following 2 h resolution at 150 V at 4 °C, the gels were transferred to nitrocellulose membrane and subjected to immunoblotting.

**Protein cross-linking and mass spectrometry.** Crosslinking was performed in buffer containing 25 mM Hepes pH 7.3, 250 mM NaCl and 2 mM DTT with or without 0.007% glutaraldehyde or 1% formaldehyde (w/v). Reactions were terminated by the addition of 3 $\times$  SDS-PAGE buffer, denatured and resolved on 10% SDS-PAGE or 4–12% gradient MES gel, respectively. Following resolution the gels were either subjected to immunoblotting with N-20 anti-Mdm2 antibody or were stained with Bio-Safe Coomassie stain (BioRad). Indicated bands were digested with trypsin and spotted on stainless steel targets with  $\alpha$ -cyano-4-hydroxycinnamic acid as described previously<sup>55</sup>. All digests were analyzed by MALDI-TOF MS with a Voyager DE-Pro mass spectrometer (Applied Biosystems) equipped with a 337-nm nitrogen laser operated in the positive ion, reflectron mode with delayed extraction over the *m/z* range of 500–4,000. Spectra were collected with 400 laser shots averaged to yield a peptide mass fingerprint. Spectra were processed using Mascot Wizard and a Mascot server (Matrix Science Ltd.) for protein identifications of Mdm2. Searches were made against the NCBI nonredundant database of 08/25/09 with human taxonomic filter (209,358 sequences). Other spectra were recorded in positive linear mode in an effort to detect weak peptide signals.

**ChIP assays and qPCR.** ChIP and qPCR analysis was carried out using p53<sup>-/-</sup>; *mdm2*<sup>-/-</sup> (2KO) cell extracts transfected with the indicated constructs as previously described<sup>56</sup>. Graphs are representative of at least three biological replicate experiments. Standard curves containing 0.1–27 ng of 2KO cell genomic DNA were run alongside the samples for each primer pair. Results were analyzed by the absolute quantification method. Error bars indicate the s.d. of three PCR amplifications of one experiment. Primer sequences are as follows: insulin exon2, F: TGGCTTCTTCTACACACCCAAG; insulin exon2, R: ACAATGCCACGCTTCTGC; p21 5' distal p53 binding site: F: TGGCCTTCAGGAACATGTCTT, R: CACCACCCTGCACTGAAGC.

**Peptide synthesis.** All peptides were synthesized on Rink amide MBHA resin on a Liberty microwave-assisted peptide synthesizer (CEM) using standard Fmoc (9-fluorenylmethoxycarbonyl) chemistry. Tryptophan was added at the peptides' N termini for UV spectroscopy. The peptides were purified on a Gilson high-pressure liquid chromatography using a reverse-phase C8 semi-preparative column (ACE) with a gradient from 5% to 60% acetonitrile in water (both containing 0.001% (v/v) trifluoroacetic acid).

Cell lines, transfections, immunoblotting and protein purification are described in **Supplementary Methods**.

52. Lokshin, M., Li, Y., Gaidon, C. & Prives, C. p53 and p73 display common and distinct requirements for sequence specific binding to DNA. *Nucleic Acids Res.* **35**, 340–352 (2007).
53. Zhang, T. & Prives, C. Cyclin a-CDK phosphorylation regulates MDM2 protein interactions. *J. Biol. Chem.* **276**, 29702–29710 (2001).
54. Rotem, S. *et al.* The structure and interactions of the proline-rich domain of ASPP2. *J. Biol. Chem.* **283**, 18990–18999 (2008).
55. Cardinale, C.J. *et al.* Termination factor Rho and its cofactors NusA and NusG silence foreign DNA in *E. coli*. *Science* **320**, 935–938 (2008).
56. Beckerman, R. *et al.* A role for Chk1 in blocking transcriptional elongation of p21 RNA during the S-phase checkpoint. *Genes Dev.* **23**, 1364–1377 (2009).